

Regulation of acid-base transporters by reactive oxygen species following mitochondrial fragmentation

David Johnson, Erik Allman and Keith Nehrke

Am J Physiol Cell Physiol 302:C1045-C1054, 2012. First published 11 January 2012;
doi:10.1152/ajpcell.00411.2011

You might find this additional info useful...

This article cites 56 articles, 27 of which can be accessed free at:

<http://ajpcell.physiology.org/content/302/7/C1045.full.html#ref-list-1>

Updated information and services including high resolution figures, can be found at:

<http://ajpcell.physiology.org/content/302/7/C1045.full.html>

Additional material and information about *AJP - Cell Physiology* can be found at:

<http://www.the-aps.org/publications/ajpcell>

This information is current as of April 23, 2012.

Regulation of acid-base transporters by reactive oxygen species following mitochondrial fragmentation

David Johnson,^{1*} Erik Allman,^{2*} and Keith Nehrke^{2,3}

Departments of ¹Biomedical Genetics, ²Pharmacology and Physiology, and ³Medicine, University of Rochester Medical Center, Rochester, New York

Submitted 17 November 2011; accepted in final form 6 January 2012

Johnson D, Allman E, Nehrke K. Regulation of acid-base transporters by reactive oxygen species following mitochondrial fragmentation. *Am J Physiol Cell Physiol* 302: C1045–C1054, 2012. First published January 11, 2012; doi:10.1152/ajpcell.00411.2011.—Mitochondrial morphology is determined by the balance between the opposing processes of fission and fusion, each of which is regulated by a distinct set of proteins. Abnormalities in mitochondrial dynamics have been associated with a variety of diseases, including neurodegenerative conditions such as Alzheimer's disease, Parkinson's disease, and dominant optic atrophy. Although the genetic determinants of fission and fusion are well recognized, less is known about the mechanism(s) whereby altered morphology contributes to the underlying pathophysiology of these disease states. Previous work from our laboratory identified a role for mitochondrial dynamics in intracellular pH homeostasis in both mammalian cell culture and in the genetic model organism *Caenorhabditis elegans*. Here we show that the acidification seen in mutant animals that have lost the ability to fuse their mitochondrial inner membrane occurs through a reactive oxygen species (ROS)-dependent mechanism and can be suppressed through the use of pharmacological antioxidants targeted specifically at the mitochondrial matrix. Physiological approaches examining the activity of endogenous mammalian acid-base transport proteins in rat liver Clone 9 cells support the idea that ROS signaling to sodium-proton exchangers contributes to acidification. Because maintaining pH homeostasis is essential for cell function and viability, the results of this work provide new insight into the pathophysiology associated with the loss of inner mitochondrial membrane fusion.

mitochondria dynamics; pH regulation; *Opal*; *Caenorhabditis elegans*

CELLS POSSESS AN ARRAY of proteins that are responsible for manipulating the structure of mitochondria. Whereas a vast number of proteins can affect the structure of the mitochondrial network (24), there are a few core proteins that are directly involved in the joining and dividing of mitochondria. In humans these are the cytosolic dynamin-related GTPase DRP1 and its outer membrane-bound adapter protein, hFIS1, which mediate the fission process, and their counterparts, the outer membrane GTPases MFN1 and MFN2 (mitofusins) and the inner membrane GTPase OPA1, which control the fusion process (2, 13, 20, 22, 25, 32, 39, 44, 45, 49, 57). These proteins are highly conserved from yeast to human, indicating that they were established early in evolution.

These alterations to mitochondrial architecture are not superficial in nature, but rather are important to a number of physiological processes, including maintenance of a healthy mitochondrial population (54), mitochondrial trafficking (4,

23), and apoptosis (16). The contribution of mitochondrial fusion to human health is underscored by the fact that mutation in the *Mfn2* and *Opal* genes has been identified as the genetic cause of Charcot-Marie-Tooth syndrome type 2A (CMT2A) and autosomal dominant optic atrophy (ADOA), respectively (13, 58). Despite knowing the genetic determinants of these diseases, how their loss contributes to pathophysiological output is an evolving question. Homozygous null mutation of these genes in mammals is lethal, but recently, a nematode model has been established that allows the *in vivo* study of how reduced mitochondrial fusion influences organismal and cellular physiology (26).

In the nematode *Caenorhabditis elegans*, mitochondrial fusion is controlled by the inner mitochondrial membrane GTPase EAT-3 (OPA1) and the outer mitochondrial membrane GTPase FZO-1 (MFN1/2) (28). We have previously demonstrated that chronic fragmentation of the mitochondrial network causes intracellular acidification in both *C. elegans* and mammalian cells (26). Moreover, we reported that the loss of outer mitochondrial membrane (OMM) fusion results in lactic acidosis, whereas the loss of inner mitochondrial membrane (IMM) fusion occurs independently of lactic acidosis but can be suppressed by treatment with the antioxidant compound *N*-acetylcysteine (NAC). This is consistent with a heightened sensitivity to the oxidant paraquat (28) and demonstrable oxidation of the mitochondrial matrix in these worms (26), leading to the hypothesis that oxidative signaling may underlie acidification following loss of IMM fusion.

Maintaining intracellular pH homeostasis is undoubtedly complex. Although both metabolism and environment are contributing factors, pH balance is generally determined by the activity of membrane transport proteins that carry acid-base equivalents. Several studies have established the ability of reactive oxygen species (ROS) such as H₂O₂ and *t*-butyl hydroperoxide (tBOOH) to affect mammalian acid-base transporters both acutely and chronically (1, 11, 29, 33). In particular, acute treatment with H₂O₂ following the imposition of an acid-load inhibits the activity of the ubiquitous sodium-proton exchanger NHE1, leading to cellular acidification and eventually death (1, 29, 33). However, the mechanisms through which this occurs are still under investigation.

Na⁺/H⁺ exchangers are only one facet of a complex homeostatic system that is required to maintain physiological intracellular pH (pH_i). Other classes of membrane transport proteins, in particular those permeable to bicarbonate, comprise another facet. These include the sodium-bicarbonate transporters (NBC) and chloride-bicarbonate exchangers (AE). Both of these classes of proteins have been shown to be sensitive to oxidative stress in mammalian systems (5, 12, 41, 46), and their activities may respond to mitochondrial damage

* D. Johnson and E. Allman contributed equally to this work.

Address for reprint requests and other correspondence: K. Nehrke, Dept. of Medicine, Nephrology Division, Univ. of Rochester Medical Center Box 675, 601 Elmwood Ave., Rochester NY 14642 (e-mail: keith_nehrke@urmc.rochester.edu).

(30). Yet, to date, the relationships between mitochondrial dynamics, oxidative stress, and pH homeostasis have not been explored.

Here, both *C. elegans* and mammalian cell culture models were used to test the hypothesis that ROS acts as a molecular trigger to induce the acidification observed in animals and cells lacking IMM fusion. Our results support the conclusion that ROS signaling in fragmented mitochondria acts through the modification of membrane acid-base transporter activities, mainly that of Na⁺/H⁺ exchangers, leading to cellular acidosis.

MATERIALS AND METHODS

Strains and plasmid constructs. Standard culture techniques were used to maintain nematodes at 20°C on normal growth medium-agar plates (8). For imaging studies, the worms were transferred to plates with agarose substituted for agar to reduce background fluorescence. The wild-type strain is Bristol N2. All of the mutants described in this work have been back-crossed to N2 Bristol at least three times before use. The *nhx-4(ok668)* strain was created by the *C. elegans* Gene Knockout Consortium. The *eat-3(tm1107)* and *fzo-1(tm1133)* alleles were generated by Dr. Shohei Mitani with the Japanese Biosource Project, and the *eat-3(ad426)* strain was created by Dr. Leon Avery. Strains were obtained from the *C. elegans* Genetics Center (University of Minnesota), and Dr. Alex van der Bliek (University of California at Los Angeles) generously provided several of the mutants as back-crossed strains.

Strains expressing the pH-sensitive green fluorescent protein (GFP) variant pHluorin or the mitochondria targeted redox sensor roGFP (21) have been previously described (26). Biosensors were crossed into mutant strains using standard mating techniques. For *nhx-4* crosses, single-worm genomic PCR was used to discriminate between the wild-type and mutant alleles with primers designed and annotated by the *C. elegans* Gene Knockout Consortium.

The strains used in this work are N2-Bristol; KWN26 *pha-1(e2123ts)III*, myEx006 [pIA5-*nhx-2* (*Pnhx-2::pHluorin*), pCL1 (*pha-1+*)]; KWN47 *eat-3(ad426)II*, *pha-1(e2123ts)III* myEx006; KWN62 *eat-3(tm1107)II*, *pha-1(e2123ts)III* myEx006; KWN67 *pha-1(e2123ts)III*, *him-5(e1490)V* myEx034 [pDJ4 (*Pmyo-3::pHluorin*), pCL1 (*pha-1+*)]; KWN119 *pha-1(e2123ts)III*, *him-5(e1490)V* myEx061 [pDJ7 (*Pmyo-3::mito-roGFP*), pCL1 (*pha-1+*)]; KWN154 *eat-3(ad426)II*, *pha-1(e2123ts)III*, *him-5(e1490)V* myEx034; KWN155 *eat-3(tm1107)II*, *pha-1(e2123ts)III*, *him-5(e1490)V* myEx034; KWN156 *eat-3(ad426)II*, *pha-1(e2123ts)III*, *him-5(e1490)V* myEx061; KWN214 *nhx-4(ok668)X*, *pha-1(e2123ts)III*, *him-5(e1490)V* myEx034; KWN390 *eat-3(ad426)II*; KWN391 *eat-3(tm1107)II*; KWN392 *fzo-1(tm1133)II*; and KWN393 *eat-3(ad426)II*, *nhx-4(ok668)X*, *pha-1(e2123ts)III*, *him-5(e1490)V* myEx034.

Tissue culture. Clone 9 rat liver cells were maintained in F-12K medium (GIBCO) containing phenol red, 2.5% sodium bicarbonate, 10% FBS (Atlanta Biologicals), and 1× penicillin-streptomycin. For experiments, the cells were diluted and transferred to 6-well tissue culture dishes containing 12-mm acid-washed glass coverslips and grown to 70–80% confluence, followed by transfection with scrambled or *Opal* short interfering (si)RNA (Integrated DNA Technologies) using Oligofectamine reagent (Invitrogen). After 2 days of exposure to *Opal* siRNA, one of the coverslips was treated with MitoTracker red CMXRos (Invitrogen) to confirm mitochondrial fragmentation.

AP-1 cells, a Chinese hamster ovary cell line lacking endogenous NHE activity, were maintained in DMEM-F12 (1:1; GIBCO) containing phenol red, 10% FBS (Atlanta Biologicals), and 1× penicillin-streptomycin. Cells were cultured as described above and transfected with an NHX-4 V5 epitope-tagged transgene (p3Dnhx-4a) and CD8 as a comarker (pID3-CD8 vector at 1:5) using Lipofectamine LTX

reagent (Invitrogen). After 24 h, Na⁺/H⁺ exchange activity was measured in anti-CD8 bead (DynaL Biotech)-reactive cells as detailed below.

pH and redox imaging in *C. elegans*. Transgenic nematodes were imaged live and unrestrained on a 60-mm nematode growth medium (NGM)-agarose plate lightly seeded with OP50 bacteria via a high-NA ×20 Nikon Plan Apo objective with fluorescent emissions monitored at 535 nm following high-speed dual excitation at 410 and 470 nm. Illumination was provided by a Polychrome V monochromator (TILL Photonics, Munich, Germany) rigged to a Nikon Eclipse TE2000-S inverted microscope equipped with a high-speed charge-coupled device camera (Cooke, Kelheim, Germany). To generate absolute pH values, the ratio of emission values was plotted against an in situ high K⁺-nigericin calibration curve as described previously (52). The redox status was presented as a ratio that was normalized to untreated wild-type N2 controls. Ten to 30 hermaphrodite nematodes were imaged per experiment.

Measurements of acid-base transport activity. To measure pHi, cells were loaded with the pH-sensitive vital dye BCECF-AM (2 μM final) for 15 min in the physiological saline solution MEH containing (in mM) 135 NaCl, 5.4 KCl, 0.4 KH₂PO₄, 0.33 NaH₂PO₄, 10 glucose, 20 HEPES, 1.2 CaCl₂, and 0.8 MgSO₄, with pH adjusted to 7.4 with Tris base. The cells were then placed into a perfusion chamber containing MEH under a high-NA ×10 air objective on the imaging rig described above. Sequential 10-ms exposures were obtained at 490- and 440-nm excitation wavelengths, and the ratio of emissions at 535 nm was converted to pH via a high K⁺-nigericin calibration curve (52).

To measure NHE activity, an ammonium prepulse technique was used. Briefly, cells were exposed to MEH containing 30 mM NH₄⁺ for 15 min and then to Na⁺-free MEH containing 135 mM *N*-methyl-D-glucamine (NMDG) for 5 min. Subsequent exposure to MEH allowed pH_i recovery to occur through Na⁺/H⁺ exchange activity, which was confirmed by its 5-ethylisopropyl amiloride (EIPA) sensitivity. The rate of NHE activity was calculated at pH 6.5 using linear regression of a plot of pH vs. change in pH (ΔpH) during the initial recovery.

For NBC activity, Na⁺-dependent pH recovery from respiratory acidosis was measured in HCO₃⁻-buffered solution in the presence of EIPA to inhibit NHE activity. For AE activity, the rate of alkalinization on removal of Cl⁻ from HCO₃⁻-buffered solution was measured. All HCO₃⁻ buffers contained (in mM) 133.1 Na⁺, 4.6 K⁺, 0.6 Mg²⁺, 0.30 Ca²⁺, 10 HEPES, 6 glucose, 25 HCO₃⁻, 106.6 Cl⁻, 1.7 phosphate, 5 OH⁻, 0.6 sulfate, and 0.001 EIPA. Na⁺ was substituted with a combination of NMDG and choline salts, and Cl⁻ was substituted with gluconate salts where stated. All solutions were isotonicly balanced and were bubbled with 5% CO₂ to a pH of ~7.4 just before use. A microelectrode was used to confirm that the pH of the buffer in the chamber remained at 7.4 during perfusion. Rates were calculated from linear regression of a plot of pH vs. time during the initial recovery.

Confocal microscopy. Confocal micrographs were taken on an Olympus IX81 inverted laser scanning confocal microscope. Images were taken using a ×100 oil objective. Z stacks ranging from 5–30 slices were taken for each specimen examined. Olympus Fluoview1000 software was used to predict optimal slice thickness and for post hoc image processing and analysis.

Antioxidant supplementation. Worms were grown on NGM plates containing 5 mM 2,2,6,6-tetramethylpiperidine-*N*-oxyl-4-ol (TEMPOL) or 50 μM (2-(2,2,6,6-tetramethylpiperidin-1-oxyl-4-ylamino)-2-oxoethyl)triphenylphosphonium chloride (mito-TEMPO). Animals were transferred to plates as L3 larvae. Subsequently, pH measurements were made in their progeny when they reached the L3 larval stage as described. Similarly, siRNA-treated Clone 9 rat liver cells (24 h posttransfection) were treated with 50 or 500 μM mito-TEMPO-conditioned antibiotic-free medium for 24 h. *nhx-4*-transfected AP-1 cells (4 h posttransfection) were treated with 500 μM mito-TEMPO-conditioned antibiotic-free medium for 20 h.

Western blotting and immunohistochemistry. Western blotting was performed on scrambled control and *Opal* siRNA-treated cells 48 h after transfection as described. Cells were removed from culture dishes by mechanical disruption following 5 min of treatment with Dulbecco's PBS, transferred to a 10-ml conical tube, and spun at 1,000 *g* for 3 min, after which the supernatant was removed. Before gel loading, the protein concentration of the cell pellets was measured using a Lowry assay. Samples were then resuspended in 2× Laemmli loading buffer containing β-mercaptoethanol and boiled for 5 min before loading. Samples were separated on a 15% acrylamide gel for 2 h, after which the protein content of the gel was transferred to a nitrocellulose membrane using a Bio-Rad semidry transfer apparatus. After transfer, total protein concentration was determined via Ponceau staining for normalization. The membrane was then washed with water several times to remove Ponceau from the membrane and blocked overnight at 4°C in 5% nonfat dry milk in Tween-buffered saline containing 0.1% Triton X-100 (TBS/T). The membrane was then incubated with a rabbit-anti-OPA1 polyclonal antibody (Novus) diluted at 1:5,000 in blocking buffer and incubated at room temperature for 2 h. After three 5-min washes with TBS/T, a peroxidase-conjugated goat anti-rabbit secondary antibody (GE Pharmaceuticals) was added and incubated for 1 h at room temperature to detect OPA1 protein levels.

RESULTS

Oxidative stress causes cellular acidification in *C. elegans*. pH homeostasis is a complex process that results from balancing the activities of membrane acid loaders and acid extruders with acid production, from sources such as catabolic processes, with intracellular buffering capacity opposing changes in pH. Previously, we demonstrated that the loss of IMM fusion results in acidification that can be suppressed by antioxidant treatment, suggesting that fragmentation in this context leads to oxidative stress, which then leads to acidosis. Here, we sought to determine whether oxidative stress itself is sufficient to

cause acidification. Precedent for this idea came from observations that treating cultured mammalian cells with chemical oxidants such as H₂O₂ significantly reduced their ability to recover from an acid load (1, 11, 29).

To determine if worms are similarly susceptible to oxidative stress-induced acidification, animals were grown on medium containing the oxidative compound tBOOH for a period of 24 h. The pHi of both the intestinal cells and the body wall muscle were then measured using a genetically encoded pH biosensor termed pHluorin (3, 26, 34, 42). We asked first whether pHluorin was intrinsically sensitive to tBOOH by transfecting a pHluorin cDNA into mammalian cells in culture, clamping the cell pHi to 7.4 by the addition of a high-K⁺ buffer containing the K⁺/H⁺ ionophore nigericin, measuring the fluorescence dual-excitation ratio of pHluorin, and then adding 1 mM tBOOH and performing the same measurements after a period of 10 min. Under these conditions, the apparent pHi as measured by pHluorin was 7.36 (±0.04) before the addition of tBOOH and 7.39 (±0.04) after the addition of tBOOH. This result suggests that acute oxidative stress does not change the basic spectral properties of our biosensor.

In worms, tBOOH significantly reduced pHi in both the intestine and muscle cells (Fig. 1A) without causing increased mortality (data not shown). To determine whether this acidification was additive to that observed following loss of IMM fusion, tBOOH was applied to an *eat-3* mutant strain that we had previously shown has fragmentation-induced acidification (26). Unfortunately, these worms exhibited high levels of larval arrest and death (data not shown), likely due to a heightened susceptibility to oxidative stress (28). To what extent the combined phenotype was due to acidosis, however, remains unclear.

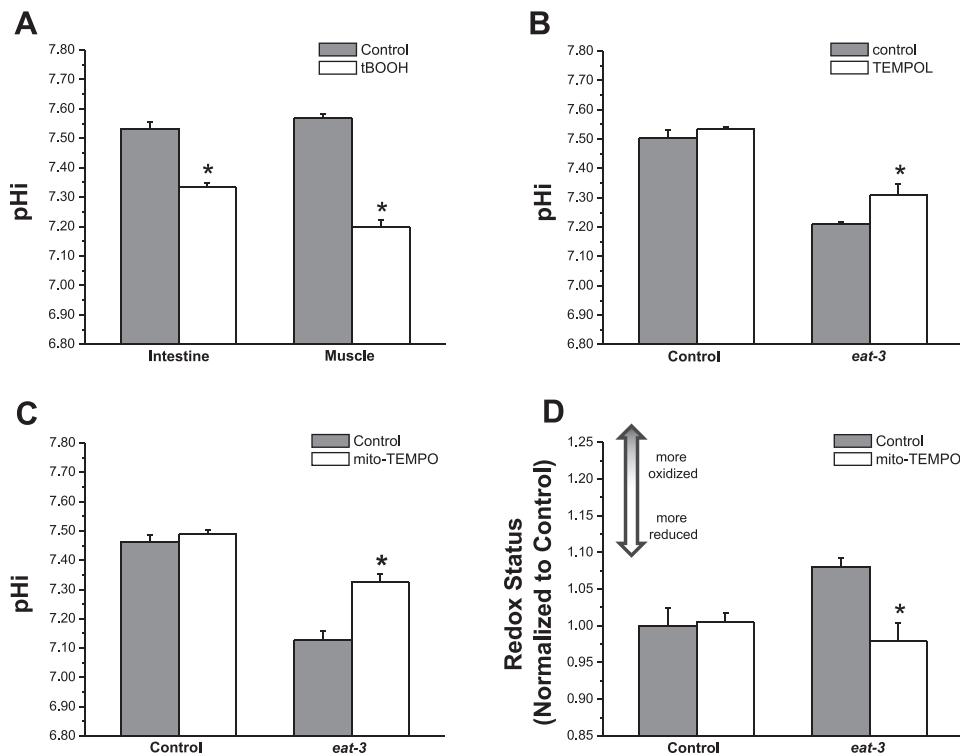


Fig. 1. Oxidative stress is sufficient to cause acidification in *Caenorhabditis elegans*: targeted antioxidants suppress mitochondrial matrix oxidation and cytosolic acidification caused by the loss of *eat-3*. **A:** wild-type worms were grown in the presence (open bars) or absence (shaded bars) of 6.2 mM *t*-butyl hydroperoxide (tBOOH) for 24 h. After treatment, cytoplasmic intracellular pH (pHi) measurements were made in the cells of the intestine and body wall muscles of freely moving transgenic worms expressing the genetically encoded fluorescent pH sensor pHluorin, as described. **B and C:** wild-type (control) and *eat-3* mutant worms were treated with the primarily cytosolic antioxidant TEMPOL (**B**) or the mitochondria-specific antioxidant mito-TEMPO (**C**) for 1 generation, and pHi was measured in the body wall muscles. **D:** mitochondrial redox status was measured in the body wall muscles of transgenic worms expressing the genetically encoded fluorescent redox sensor roGFP. The mitochondria-specific antioxidant mito-TEMPO significantly reduced the oxidation observed in *eat-3(ad426)* mutant worms. **P* < 0.01, treated vs. untreated samples. For redox and pHi measurements, values are means ± SE for 3 trials (*n* = 10–25 worms per trial).

ROS scavenging suppresses acidification in a mitochondrial fusion mutant. Because we were unable to determine whether mitochondrial fragmentation and exogenous oxidative stress were additive with respect to acidification, we asked instead whether acidosis could be suppressed by antioxidant treatment, as was suggested initially, using either NAC or catalase overexpression (26). Wild-type and mutant worms were grown on plates supplemented with the antioxidant compound TEMPOL, which has been used previously to relieve oxidative stress-induced pathologies (18, 19, 48). Worms were placed on growth medium containing 5 mM TEMPOL as L3 larvae and allowed to grow into adulthood. Intracellular pH was measured in the body wall muscles of the resulting progeny at the L3 stage of development and compared with that of mutant worms grown in the absence of the compound. Figure 1B clearly demonstrates that the body wall muscles of *eat-3* mutant worms grown in the presence of TEMPOL were less acidified than those of worms grown under control conditions, suggesting that the detoxification of cytosolic ROS is sufficient to attenuate acidification. In addition, it can be seen that TEMPOL does not alter the pH_i of control worms, confirming that the compound does not affect pH_i under normal physiological conditions. However, exposure to TEMPOL is insufficient to reverse the oxidation of the mitochondrial matrix observed in the *eat-3* mutant animals (data not shown). This is not surprising, since it has been demonstrated that TEMPOL partitions to a much greater extent in the cytosol than in intracellular compartments such as the mitochondria (53).

The mitochondrial redox environment has been shown to be more highly oxidized in *eat-3* mutants (26), suggesting that mitochondria may be the primary source of oxidative stress. Hence, we employed a TEMPOL derivative, mito-TEMPO, which is targeted to the mitochondria via a triphenylphosphonium moiety (14), and asked whether reducing mitochondrial oxidative stress was sufficient to suppress acidification. Control and *eat-3* mutant worms were grown in either the presence or absence of mito-TEMPO, and pH_i was measured in the body wall muscles of the F1 generation. The results of this experiment indicate that like TEMPOL, mito-TEMPO was able to significantly relieve the acidification normally seen in *eat-3* mutant animals (Fig. 1C). Furthermore, when the mitochondrial redox status of control and mutant worms was examined, it was found that mito-TEMPO significantly reduced the redox environment in the matrices of *eat-3* mutant mitochondria, as well (Fig. 1D). These data demonstrate that specifically relieving mitochondrial oxidative stress is sufficient to prevent the acidification caused by *eat-3* mutations. This result also supports the hypothesis that the altered redox status of *eat-3* mutant mitochondria is the result of ROS overproduction. However, ROS measurements made using the fluorescent H_2O_2 -sensitive dye dichlorofluorescein (DCF), which has been employed previously in worms (51), as well as measurements of cytosolic redox status using a genetic biosensor, suggested that wholesale ROS is not increased by loss of IMM fusion (data not shown). This is consistent with the idea that a signaling axis exists whose source is mitochondrial ROS and whose ultimate output is pH balance. With this in mind, we next sought to identify molecular targets whose activities would fit into this scheme.

Oxidative stress, mitochondrial fragmentation, and acid-base transporters: HCO_3^- transporters. Physiological acid-base homeostasis is maintained through a concerted effort among multiple classes of ion transport proteins that allow the movement of acid-base equivalents across the membrane. These proteins can act as either acid loaders or acid extruders depending on their electrolyte specificity and the direction of ion movement. In addition to protons (H^+) and hydroxyl ions (OH^-), bicarbonate (HCO_3^-) represents an important component of the pH regulatory system and is transported by several classes of proteins (for review, see Ref. 7). In the following sets of experiments, we measured how acute exogenous oxidative stress regulates NBC and AE activities in rat liver Clone 9 cells in culture. Mitochondrial fragmentation in this cell culture model has been shown to cause significant intracellular acidosis (26). All of the rate data from the physiological experiments are summarized in Table 1.

NBC activity was monitored using the pH-sensitive vital dye BCECF-AM by measuring the rate of Na^+ -dependent pH_i recovery after HCO_3^- -induced acidification (Fig. 2A). EIPA, a specific inhibitor of NHE activity, was included to eliminate NBC-independent recovery. Clone 9 cells were subjected to oxidative stress by applying three types of exogenous ROS-producing compounds. H_2O_2 and its more stable derivative, tBOOH, are substrates for catalase, whereas paraquat is thought to affect redox cycling and may be a superoxide generator. These applications were acute, with measurements being made within minutes of exposure. NBC activity was generally reduced by oxidative stress, although the effect of paraquat did not reach statistical significance (Table 1 and Fig. 2B). Because NBCs are in most cases acid extruders, reducing NBC activity would be expected to contribute to cellular acidification.

Having established the precedent that NBC activity could be reduced by exogenous oxidative stress, we next asked whether NBC activity was reduced specifically by mitochondrial fragmentation. Clone 9 cells were treated with either *Opal* or scrambled siRNA, and the efficacy of *Opal* siRNA targeting was assessed by immunoblotting. On average, OPA1 protein levels were reduced ~35% by siRNA treatment (Fig. 2C). Fluorescent images of mitochondria from *Opal* siRNA-transfected cells labeled with MitoTracker red CMXRos indicate that this reduction in OPA1 protein was sufficient to cause fragmentation (Fig. 2D). More importantly, this level of knock-down and the resulting fragmentation of the mitochondrial network have been previously shown to result in cellular acidification (26). It is not surprising that incomplete knock-down of OPA1 is enough to trigger fragmentation, since dominant optic atrophy, which results from mutation of *Opal* in humans, is a disease caused by haploinsufficiency (31). However, the results of these experiments clearly do not support a role for reduced NBC activity in contributing to fragmentation-induced acidosis (Fig. 2E). Undoubtedly, oxidative stress responses involve multiple signaling pathways, and our results suggest that a blanket application of reactive species may not recapitulate endogenous signaling cascades, particularly as regards localized ROS production such as we posit occurs during mitochondrial fragmentation.

A similar tactic was applied to measure AE regulation by oxidative stress as described above, with the caveat that Cl^- removal from the extracellular HCO_3^- -buffered medium was

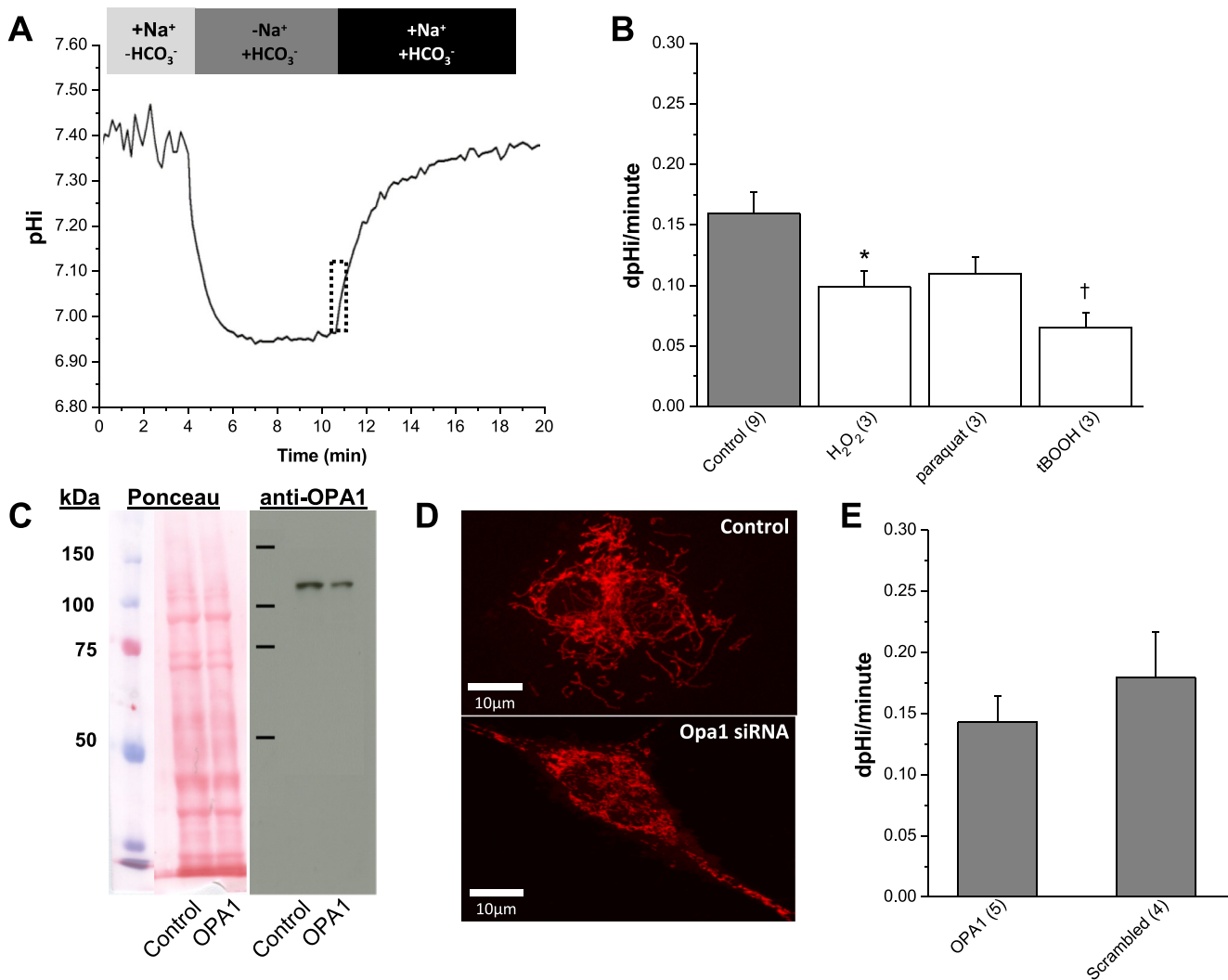


Fig. 2. $\text{Na}^+/\text{HCO}_3^-$ cotransporter (NBC) activity is reduced by ROS but not mitochondrial fragmentation in rat liver Clone 9 cells. **A:** this schematic represents the protocol used to measure NBC activity. Cells were incubated with BCECF before recording. The cells were superfused as indicated, and the addition of HCO_3^- to the superfusate was complemented with bubbling with 5% CO_2 . All solutions contained 1 μM EIPA to eliminate the activity of Na^+/H^+ exchangers. **B:** effects of ROS on NBC activity. The rate of pH change (dpHi/minute) in untreated normal cells (shaded bar) is plotted vs. experimental acute treatments with oxidants (open bars; 20-min exposure), as indicated. The rates, indicated in pH units per minute, are derived from a linear regression fit to the first minute of recovery, as denoted by the dotted box in **A**. Data are means \pm SE for n trials (in parentheses). * $P < 0.05$; † $P < 0.01$ vs. control (using 2-tailed t -test). **C:** Western blot analysis of OPA1 protein levels following short interfering (si)RNA treatment. *Left*, OPA1 protein levels were normalized to total protein detected by Ponceau staining. *Right*, OPA1 protein levels were determined in whole cell extracts 48 h posttransfection with scrambled control and *Opa1* siRNA using a rabbit anti-OPA1 antibody (Novus). **D:** confocal micrographs of mitochondria, labeled with MitoTracker red CMXRos, in control (*top*) or *Opa1* siRNA-treated cells (*bottom*). **E:** NBC activity as a function of mitochondrial fragmentation. Data are means \pm SE for n trials (in parentheses). All rate trials (n) are an average of 20–25 individual cells collected from a single field of view (FOV). Acute concentrations were 50 μM H_2O_2 , 100 μM paraquat, and 1 mM tBOOH added 20 min before recovery.

used to elicit activity. The resulting exchange of intracellular Cl^- for extracellular HCO_3^- caused a cellular alkalinization whose rate was reflective of AE activity (Fig. 3A). Our data demonstrate that acute treatment with paraquat increased AE activity by nearly 75% on average, although the P value did not quite reach significance (Fig. 3B). Because AE family transporters are acid loaders, this regulation by oxidative stress would be predicted to drive cellular acidification. However, as was the case with NBC activity, OPA1 knockdown did not increase the rate of $\text{Cl}^-/\text{HCO}_3^-$ exchange relative to the untreated cells (Fig. 3C), and hence some other mechanism must contribute to the disruption in pH homeostasis.

Oxidative stress, mitochondrial fragmentation, and acid-base transporters: Na^+/H^+ exchangers. In mammalian cells, exposure to oxidants such as H_2O_2 has been shown to cause cellular acidification by inhibiting the activity of the ubiquitous Na^+/H^+ exchanger NHE1 (15, 33, 47). To assess NHE activity in Clone 9 cells and its potential regulation by oxidative stress, an ammonium prepulse was used to trigger transient acidification and the rate of EIPA-sensitive, Na^+ -dependent recovery from this acid load was measured (Fig. 4A). As was the case for NBC activity, acute oxidative stress generally reduced NHE activity (Fig. 4B), which would favor acidification. In contrast to the results with NBC and AE activities, however, we found

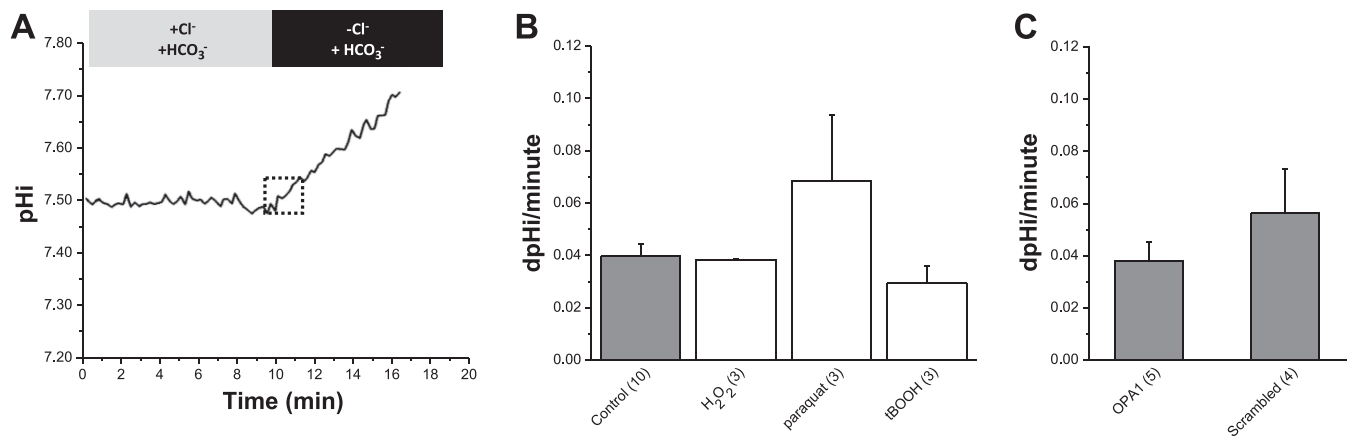


Fig. 3. $\text{Cl}^-/\text{HCO}_3^-$ exchange (AE) activity, ROS, and mitochondrial fragmentation in rat Clone 9 cells. **A:** This schematic represents the protocol used to measure AE activity. Cells were incubated with BCECF before recording. The cells were superfused as indicated in the presence of HCO_3^- and 5% CO_2 . All solutions contained 1 μM EIPA. **B:** effects of ROS on AE activity. The rate of pH change in untreated normal cells (shaded bar) is plotted vs. experimental acute treatments with oxidants (open bars; 20-min exposure), as indicated. The rates, indicated in pH units per minute, are derived from a linear regression fit to the first 3 min of recovery, as denoted by the dotted box in **A**. Data are means \pm SE for n trials (in parentheses). **C:** AE activity as a function of mitochondrial fragmentation. Data are means \pm SE for n trials (in parentheses). All rate trials (n) are an average of 20–25 individual cells collected from a single FOV. Acute concentrations were 50 μM H_2O_2 , 100 μM paraquat, and 1 mM tBOOH added 20 min before recovery.

that knockdown of OPA1 significantly reduced NHE activity relative to cells treated with scrambled control siRNA (Fig. 4C).

However, transfection of the scrambled siRNA was not without effect, and NHE activity was reduced somewhat in these cells relative to nontransfected cells (Fig. 4, **B** and **C**). There are several potential mechanisms that could account for this. First, nonspecific effects of siRNA have been noted previously and may occur through stimulation of innate immune pathways (27). Alternatively, it has been shown that treating cells with cationic lipids, such as occurs during transfection, leads to increases in ROS production (50). Support for this latter mechanism comes from data indicating that exposure to a low level of mito-TEMPO relieved the nonspecific siRNA-mediated suppression of NHE activity (Fig. 4C). Under these same conditions, however, the *Opa1* siRNA-treated cells were

still relatively acidified relative to the scrambled control cells. However, when treated with high levels of mito-TEMPO, the scrambled control and *Opa1* siRNA treated cells exhibited virtually identical levels of NHE activity (Fig. 4C). We interpret this dose dependence as reflecting two signaling pathways that operate through ROS, and we conclude that ROS produced by mitochondrial fragmentation can regulate NHE activity but that NHEs are also sensitive to oxidative stress produced by transfection with cationic lipids.

Acidification in a mitochondrial fusion mutant is not solely a consequence of inhibiting the C. elegans ubiquitous Na^+/H^+ exchanger NHX-4. *C. elegans* possess a nine-member family of Na^+/H^+ exchangers, the NHXs (NHX-1–9) (35). The *nhx* genes are generally expressed in a limited set of cells suggestive of tissue-specific roles. This is exemplified by NHX-7, whose expression is restricted to the posterior cells of the

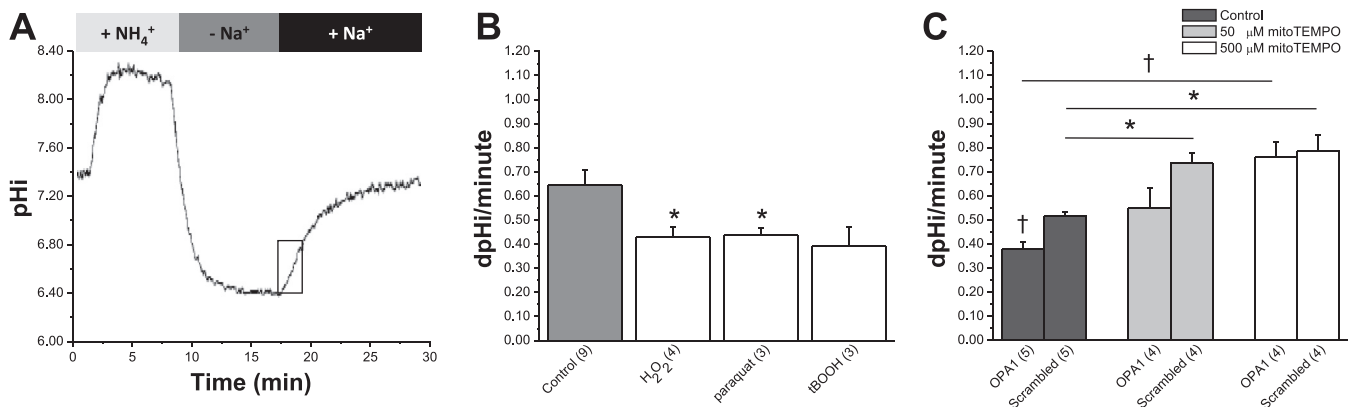


Fig. 4. Na^+/H^+ exchanger (NHE) activity is inhibited by both ROS and mitochondrial fragmentation in rat liver Clone 9 cells. **A:** this schematic represents the protocol used to measure NHE activity. Cells were incubated with BCECF before recording. **B:** effects of ROS on NHE activity. The rate of pH change in untreated normal cells (shaded bar) is plotted vs. cells treated acutely with various types of ROS (open bars; 20-min exposure), as indicated. NHE activity, indicated in pH units per minute, is derived from a linear regression of a plot of pH vs. ΔpH calculated from the region within the box in **A** and is reported as the instantaneous rate at pH 6.5. Data are means \pm SE for n trials (in parentheses). * $P < 0.05$ vs. control (using 2-tailed t -test). **C:** NHE activity as a function of mitochondrial fragmentation and antioxidant treatment. Cells were treated for 24 h with 50 or 500 μM mito-TEMPO at 24 h after siRNA transfection. * $P < 0.05$; † $P < 0.01$, vs. scrambled siRNA or between untreated and treated cells, as indicated (using 2-tailed t -test). All trials (n) are an average of 20–25 individual cells collected from a single FOV. Acute concentrations were 50 μM H_2O_2 , 100 μM paraquat, and 1 mM tBOOH added 20 min before recovery.

Table 1. Activity of acid-base transporters

Treatment	Compound	dpH _i /dt, pH unit min ⁻¹ × 10		
		Na ⁺ /H ⁺ Exchange (NHE)	Na ⁺ /HCO ₃ ⁻ Cotransport (NBC)	Cl ⁻ /HCO ₃ ⁻ Exchange (AE)
None	none	6.47 ± 0.61 (9)	1.59 ± 0.17 (9)	0.40 ± 0.05 (10)
None	EIPA§	0.06 ± 0.04‡ (3)	n.d.	n.d.
Opa1	none	3.78 ± 0.33† (5)	1.43 ± 0.21 (5)	0.38 ± 0.07 (5)
Scrambled	none	5.14 ± 0.19 (5)	1.79 ± 0.37 (4)	0.56 ± 0.17 (4)
Opa1	mito-TEMPO (50 μM)	5.50 ± 0.81 (4)	n.d.	n.d.
Scrambled	mito-TEMPO (50 μM)	7.34 ± 0.44 (4)	n.d.	n.d.
Opa1	mito-TEMPO (500 μM)	7.62 ± 0.63 (4)	n.d.	0.74 ± 0.03 (4)
Scrambled	mito-TEMPO (500 μM)	7.85 ± 0.69 (4)	n.d.	0.70 ± 0.10 (4)
None	H ₂ O ₂	4.32 ± 0.39* (4)	0.99 ± 0.13* (3)	0.38 ± 0.01(3)
None	paraquat	4.38 ± 0.31* (3)	1.10 ± 0.14 (3)	0.69 ± 0.25 (3)
None	tBOOH	3.94 ± 0.80 (3)	0.65 ± 0.12† (3)	0.29 ± 0.07 (3)
Transfection with <i>nhx-4</i>	None	2.20 ± 0.20 (8)		
Transfection with <i>nhx-4</i>	mito-TEMPO (500 μM)	2.54 ± 0.15 (4)		
Transfection with <i>nhx-4</i>	H ₂ O ₂	2.05 ± 0.14 (6)		
Transfection with <i>nhx-4</i>	tBOOH	1.61 ± 0.23 (3)		

Rates of intracellular pH change (dpH_i/dt) are means ± SE for *n* trials (in parentheses). Each rate trial (*n*) is an average of 20–25 individual cells collected from a single field of view. The rate of NHX-4 activity was measured in transiently transfected AP-1 cells, and all other measurements were made in rat liver Clone 9 cells. Na⁺/H⁺ exchange rates (×10) were calculated using linear regression of a plot of pH vs. ΔpH to determine the rate at pH 6.5. Na⁺/HCO₃⁻ cotransport rates (×10) were calculated using a linear regression fit to the first minute of recovery. Cl⁻/HCO₃⁻ exchange rates (×10) were calculated using a linear regression fit to the first 3 min of recovery. **P* < 0.05; †*P* < 0.01; ‡*P* < 0.001 vs. control (using *t*-test). EIPA and *Opa1* siRNA are compared with scrambled siRNA control. Control EIPA concentration was 1 μM. Mito-TEMPO concentration was 50 or 500 μM, as noted. Acute concentrations were 50 μM H₂O₂, 100 μM paraquat, and 1 mM tBOOH added 20 min before recovery. n.d., Not determined. §Note that the EIPA rate (×10) is represented as the average instantaneous change in pH_i during the first minute of recovery, since the best fit line method cannot be applied when the slope is zero.

intestine where intestinal calcium signaling triggers it to secrete protons, signaling the overlying posterior body wall muscles to contract (42). In contrast, NHX-4 is expressed throughout the soma (35) and may be an ortholog of the ubiquitous mammalian NHE1 isozyme. The broad expression of *nhx-4* would appear to position it to respond appropriately to mitochondrial fragmentation, as mitochondria are present in all cells, and we have demonstrated that fragmentation of the mitochondrial network results in acidification of epithelial cells, muscle, and neurons in worms (26). A series of reasonable questions to ask, then, is whether NHX-4 also has a housekeeping function in maintaining pH homeostasis, and if so, whether NHX-4 transporter activity is regulated by ROS

and whether this regulation of NHX-4 might contribute to acidification following mitochondrial fragmentation in worms.

To answer the latter question, a transgene containing the *nhx-4* cDNA was expressed in AP-1 cells, which lack endogenous Na⁺/H⁺ exchange activity (43). After acidification via an ammonium prepulse, cells transfected with the *nhx-4* transgene exhibited Na⁺-dependent pH_i recovery (Fig. 5A). To explore the sensitivity of NHX-4 to oxidative stress, either 50 μM H₂O₂ or 1 mM tBOOH was added before and during the recovery period. The resulting data suggested that NHX-4 in this context was not particularly sensitive to oxidative stress (Fig. 5A). In addition, NHE activity in NHX-4-expressing cells treated with mito-TEMPO was nearly indistinguishable from

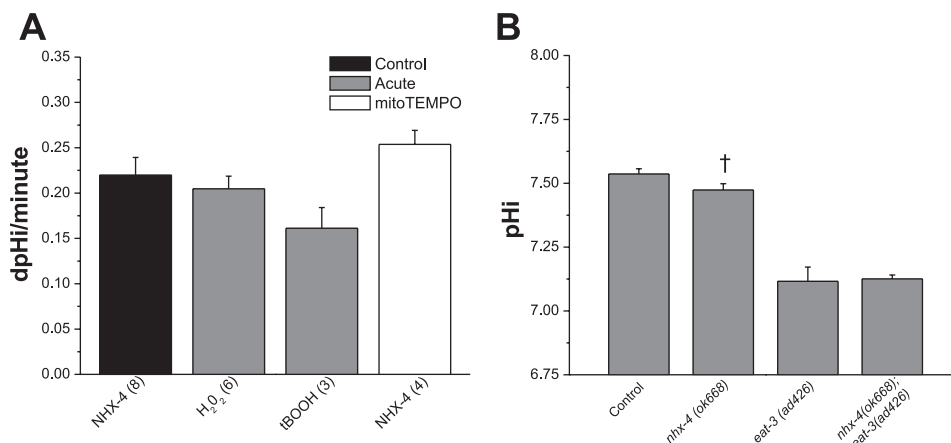


Fig. 5. The ubiquitous nematode Na⁺/H⁺ exchanger NHX-4. *A*: effects of ROS on recombinant *C. elegans* NHX-4 activity in AP-1 cells, which lack endogenous NHE activity. The rate of pH change in untreated cells (solid bar) is plotted vs. cells treated acutely with compounds to induce (shaded bars; 20-min exposure) or relieve oxidative stress (open bar; 20-h exposure), as indicated. The rates, indicated in pH units per minute at a pH of 6.5, are derived from a linear regression of plot of pH vs. ΔpH. Data are means ± SE for *n* trials (in parentheses). Each trial (*n*) is an average of 20–25 individual cells collected from a single FOV. Acute concentrations were 50 μM H₂O₂ and 1 mM tBOOH added 20 min before recovery. Cells were treated for 20 h with 500 μM mito-TEMPO at 4 h posttransfection. *B*: resting pH was measured in the body wall muscle of N2 control and mutant worms using targeted pHluorin, as indicated. Data are means ± SE for 3 trials with *n* = 15–20 worms per trial.

that in untreated cells, suggesting that the cells are not under endogenous oxidative stress. Despite this finding, it remained possible that NHX-4 could respond to stress signaling that occurs as a result of mitochondrial fragmentation in a more native context.

To directly assess the role of NHX-4 in maintaining pH homeostasis in worms, an *nhx-4* mutant allele (*ok668*) was obtained from the *C. elegans* Gene Knockout Consortium. The pH biosensor pHluorin was expressed in the body wall muscle of the *nhx-4* mutant via the *myo-3* promoter, and pH measurements were made in live, unrestrained worms expressing the biosensor. The results indicated that the pH_i of body wall muscle in the *nhx-4(ok668)* mutant was slightly reduced compared with that of control wild-type worms. Although this change was small, it was also statistically significant, supporting a role for NHX-4 in maintaining pH homeostasis. However, the degree of acidification was not as severe as that observed in the *eat-3(ad426)* mutant (Fig. 5B), leading us to conclude that any potential reduction in NHX-4 activity was not sufficient to explain the cellular acidosis observed with mitochondrial fragmentation. Moreover, the body wall muscle pH in a mutant strain lacking both *nhx-4* and *eat-3* was nearly identical to that of the *eat-3(ad426)* mutant alone (Fig. 5B). Together, these results suggest that mitochondrial fragmentation in worms is likely to involve coordinate regulation of multiple acid-base transporters.

DISCUSSION

Mitochondrial fragmentation caused by a loss of IMM fusion has been shown to result in a lactate-independent cellular acidification that is partly suppressed by NAC, an antioxidant, as well as the presence of a more highly oxidized mitochondrial matrix (26). In addition, previous evidence has demonstrated that worms lacking the ability to fuse their IMM exhibit increased vulnerability to oxidative stress itself (28). Together, these studies led us to postulate that loss of IMM fusion and the resulting mitochondrial fragmentation may result in oxidative signaling mechanisms that regulate acid-base transport proteins that are necessary to maintain pH homeostasis. In fact, there has recently been increased interest in the role of proton handling in many types of cancers, and cancerous cells appear to express specific gene products that facilitate growth under acidotic conditions (for review see Refs. 9, 37). Because mitochondrial dysfunction has been implicated in a variety of disease pathologies, and the loss of IMM fusion is associated specifically with certain types of diseases, alteration in pH homeostasis may also contribute to mitochondrial disease etiology.

In addition to demonstrating that oxidative stress can induce acidification in the worm model, we went on to show that the application of an antioxidant with superoxide and alkyl scavenging properties could reduce the extent of acidification associated with mitochondrial fragmentation. These data demonstrate the causality of ROS for acidification. Perhaps the most intriguing aspect of this work, however, is the finding that mitochondrial fragmentation regulates membrane acid-base transporters and, in the case of NHEs, that scavenging mitochondrial ROS suppresses this mode of regulation. Within that context, it was particularly interesting to discover that the fusion mutant did not produce more global ROS as detected by DCF staining (data not shown). This observation, combined

with the fact that cytoplasmic ROS scavenging partially suppressed acidification even though it did not restore redox balance in the mitochondria, suggested that localized, rather than global increases in ROS form the core of this signaling axis between the mitochondria and acid-base transporters. Perhaps this is not surprising, since global increases in cellular ROS would likely have severe negative consequences to cellular health and would lead to activation of oxidative stress response pathways, as well; moreover, specific and localized ROS-based communication between the mitochondria and other cellular compartments is not unprecedented. For example, the proapoptotic protein $p66^{Sbc}$ uses an ROS-based mechanism to promote cell death by upregulating superoxide production (38). In response to proapoptotic cues, $p66^{Sbc}$ is activated and oxidizes cytochrome *c* within the mitochondria, leading to an increase in H_2O_2 , which then acts as an intracellular messenger between the mitochondrion and nucleus. Once inside the nucleus, the H_2O_2 promotes Akt-based inhibition of FOXO3, preventing the activation of various oxidative stress response genes promoting ROS-based apoptosis (36). In addition, NADPH oxidases (NOX) promote ROS formation that triggers the activation of specific signaling cascades, including the cytokine-dependent activation of NF- κ B and the activation of hypoxic response pathways via Ras/ERK, JNK, Akt, and possibly p38/MAPK (10, 17, 40, 56).

In an attempt to tie mitochondrial ROS to transporter regulation, we applied several types of compounds to elicit global oxidative stress and examined acute regulation of three types of acid-base transporter activities. Although mitochondria generate superoxide, the activity of SOD rapidly converts superoxide to H_2O_2 , which is membrane permeable and can diffuse into the cytoplasm. Hence, we chose to examine H_2O_2 , tBOOH (a more stable version of H_2O_2), and paraquat, which has been described as a superoxide generator. These compounds are likely to trigger endogenous signaling cascades that have been well described as being involved in oxidative stress responses, such as protection against infectious agents, initiation of transcriptional factors, and eliciting antitumorigenic responses by evoking cellular senescence or even apoptosis. Although characterizing the relevant molecular components of the oxidative signaling cascade is well beyond the scope of this work, we would like to emphasize that the mechanism of transporter regulation by mitochondrial fragmentation, while undoubtedly a result of ROS signaling, does not necessarily utilize the same signal transduction pathway as that triggered by global oxidative stress. In fact, it will be quite intriguing to figure out which stress signaling pathways respond to endogenous oxidative stress, because these are more likely to be critical for disease pathogenesis.

Our understanding of how signals derived from mitochondria are communicated through the cell is still evolving, but even under basal conditions mitochondria are the major source of ROS in the cell, and thus these signaling mechanisms are likely to be important under physiological as well as pathophysiological conditions. For example, recent evidence shows that mitochondria in all cell types spontaneously emit flashes of ROS that occur more frequently under certain pathological conditions, for instance, during ischemia reperfusion (55). The mechanism by which the flashes occur appears to be linked to a transient opening of the mitochondrial permeability transition

pore (mPTP) and is dependent on a functional electron transport chain.

Although our results clearly show that mitochondrial fragmentation can regulate transporter function, an epistasis analysis between the fusion mutant *eat-3(ad426)* and the ubiquitous Na^+/H^+ exchanger mutant *nhx-4(ok668)* did not support the idea that oxidative stress could inhibit exchanger activity in a manner sufficient to explain the observed acidification. Instead, *nhx-4* may act in a permissive fashion that requires the parallel inhibition of other acid-base transporters. Therefore, it would be useful to integrate our findings with studies of other worm acid-base transporters, including NBCs and AEs, to fully understand this model of regulation. It may be similarly compelling to utilize the power of the worm as a genetic model for interrogating molecular signaling components that regulate transport downstream of mitochondrial morphology or function. However, it is important to remember that although worm and mammalian models are remarkably similar in many respects, it is possible that fragmentation causes acidification through different mechanisms in each. Although we found no role for NHX-4 in fragmentation-induced acidification, it nevertheless would be interesting to ask how cells derived from an NHE1 knockout mouse (6) respond to mitochondrial fragmentation.

In summary, the loss of IMM fusion capability in worms causes cellular acidification that can be suppressed by treatment with both cytosolic and mitochondria-specific antioxidants, implicating ROS in the progression of the phenotype. In mammalian cells in culture, a similar loss of fusion capabilities significantly reduces NHE activity, and this can be alleviated through mitochondria-specific antioxidant treatment. In general, the response of mammalian acid-base transporters to oxidative stress appears to encourage acidification; that is, acid-loaders are stimulated and acid-extruders are inhibited. In fact, it is likely that signaling through multiple transporters contributes to acidification. Because not all cells express the same repertoire of transporters, the particulars of the signaling axis may depend on context and their relative importance for maintaining pH homeostasis in a given cell or organ. In addition, specific energy demands in various cell types or pathologies can further impact ROS production, which may make certain cell types more susceptible to pH dysregulation and exacerbate the progression of disease states. Consideration of these differences may be important for understanding how oxidative stress and/or mitochondrial dysfunction contribute to disease etiology. Together, the data described in this report present a strong case for the involvement of ROS in the acidification caused by the loss of IMM fusion in both worms and mammals. In particular, they support the role of intracellular acidification in the progression of diseases related to mitochondrial morphology such as CMT2A and ADOA.

ACKNOWLEDGMENTS

We acknowledge the *C. elegans* Gene Knockout Consortium, the Japanese Bioresource Project, and the *C. elegans* Genetic Center for strains. We also thank Teresa Sherman for expert technical assistance.

GRANTS

This work was supported in part by funding from National Institute of Neurological Disorders and Stroke Grant R01 NS064945 and National Science Foundation Grant IOS0919848 (to K. Nehrke), Ruth L. Kirschstein National Research Service Award (NRSA) Institutional Training Grant T32 GM068411

(to E. Allman), and Ruth L. Kirschstein NRSA Pre-Doctoral Fellowship F31 GM084506 (to D. Johnson).

DISCLOSURES

No conflicts of interest, financial or otherwise, are declared by the author(s).

AUTHOR CONTRIBUTIONS

Author contributions: D.J., E.A., and K.N. conception and design of research; D.J. and E.A. performed experiments; D.J. and E.A. analyzed data; D.J., E.A., and K.N. interpreted results of experiments; D.J. and E.A. prepared figures; D.J. and E.A. drafted manuscript; D.J., E.A., and K.N. edited and revised manuscript; D.J., E.A., and K.N. approved final version of manuscript.

REFERENCES

1. Akram S, Teong HF, Fliegel L, Pervaiz S, Clement MV. Reactive oxygen species-mediated regulation of the Na^+/H^+ exchanger 1 gene expression connects intracellular redox status with cells' sensitivity to death triggers. *Cell Death Differ* 13: 628–641, 2006.
2. Alexander C, Votruba M, Pesch UE, Thiselton DL, Mayer S, Moore A, Rodriguez M, Kellner U, Leo-Kottler B, Auburger G, Bhattacharya SS, Wissinger B. OPA1, encoding a dynamin-related GTPase, is mutated in autosomal dominant optic atrophy linked to chromosome 3q28. *Nat Genet* 26: 211–215, 2000.
3. Allman E, Johnson D, Nehrke K. Loss of the apical V-ATPase α -subunit VHA-6 prevents acidification of the intestinal lumen during a rhythmic behavior in *C. elegans*. *Am J Physiol Cell Physiol* 297: C1071–C1081, 2009.
4. Anesti V, Scorrano L. The relationship between mitochondrial shape and function and the cytoskeleton. *Biochim Biophys Acta* 1757: 692–699, 2006.
5. Asha Devi S, Shiva Shankar Reddy CS, Subramanyam MV. Oxidative stress and intracellular pH in the young and old erythrocytes of rat. *Biogerontology* 10: 659–669, 2009.
6. Bell SM, Schreiner CM, Schultheis PJ, Miller ML, Evans RL, Vorhees CV, Shull GE, Scott WJ. Targeted disruption of the murine Nhe1 locus induces ataxia, growth retardation, and seizures. *Am J Physiol Cell Physiol* 276: C788–C795, 1999.
7. Boron WF. Regulation of intracellular pH. *Adv Physiol Educ* 28: 160–179, 2004.
8. Brenner S. The genetics of *Caenorhabditis elegans*. *Genetics* 77: 71–94, 1974.
9. Chiche J, Brahimi-Horn MC, Pouyssegur J. Tumour hypoxia induces a metabolic shift causing acidosis: a common feature in cancer. *J Cell Mol Med* 14: 771–794, 2010.
10. Cucoranu I, Clempus R, Dikalova A, Phelan PJ, Ariyan S, Dikalov S, Sorescu D. NAD(P)H oxidase 4 mediates transforming growth factor- β 1-induced differentiation of cardiac fibroblasts into myofibroblasts. *Circ Res* 97: 900–907, 2005.
11. Daskalopoulos R, Korcok J, Farhangkhgoee P, Karmazyn M, Gelb AW, Wilson JX. Propofol protection of sodium-hydrogen exchange activity sustains glutamate uptake during oxidative stress. *Anesth Analg* 93: 1199–1204, 2001.
12. De Giusti VC, Garciarena CD, Aiello EA. Role of reactive oxygen species (ROS) in angiotensin II-induced stimulation of the cardiac $\text{Na}^+/\text{HCO}_3^-$ cotransport. *J Mol Cell Cardiol* 47: 716–722, 2009.
13. Delettre C, Lenaers G, Griffoin JM, Gigarel N, Lorenzo C, Belenguer P, Pelloquin L, Grosgeorge J, Turc-Carel C, Perret E, Astarie-Dequeker C, Lasquelles L, Arnaud B, Ducommun B, Kaplan J, Hamel CP. Nuclear gene OPA1, encoding a mitochondrial dynamin-related protein, is mutated in dominant optic atrophy. *Nat Genet* 26: 207–210, 2000.
14. Dikalova AE, Bikineyeva AT, Budzyn K, Nazarewicz RR, McCann L, Lewis W, Harrison DG, Dikalov SI. Therapeutic targeting of mitochondrial superoxide in hypertension. *Circ Res* 107: 106–116, 2010.
15. Elsing C, Voss A, Herrmann T, Kaiser I, Huebner CA, Schlenker T. Oxidative stress reduces Na^+/H^+ exchange (NHE) activity in a biliary epithelial cancer cell line (Mz-Cha-1). *Anticancer Res* 31: 459–465, 2011.
16. Frank S, Gaume B, Bergmann-Leitner ES, Leitner WW, Robert EG, Catez F, Smith CL, Youle RJ. The role of dynamin-related protein 1, a mediator of mitochondrial fission, in apoptosis. *Dev Cell* 1: 515–525, 2001.

17. Gorin Y, Ricono JM, Kim NH, Bhandari B, Choudhury GG, Abboud HE. Nox4 mediates angiotensin II-induced activation of Akt/protein kinase B in mesangial cells. *Am J Physiol Renal Physiol* 285: F219–F229, 2003.
18. Hahn SM, Mitchell JB, Shacter E. Tempol inhibits neutrophil and hydrogen peroxide-mediated DNA damage. *Free Radic Biol Med* 23: 879–884, 1997.
19. Haj-Yehia AI, Nassar T, Assaf P, Nassar H, Anggard EE. Effects of the superoxide dismutase-mimic compound TEMPOL on oxidant stress-mediated endothelial dysfunction. *Antioxid Redox Signal* 1: 221–232, 1999.
20. Hales KG, Fuller MT. Developmentally regulated mitochondrial fusion mediated by a conserved, novel, predicted GTPase. *Cell* 90: 121–129, 1997.
21. Hanson GT, Aggeler R, Oglesbee D, Cannon M, Capaldi RA, Tsien RY, Remington SJ. Investigating mitochondrial redox potential with redox-sensitive green fluorescent protein indicators. *J Biol Chem* 279: 13044–13053, 2004.
22. Hermann GJ, Thatcher JW, Mills JP, Hales KG, Fuller MT, Nunnari J, Shaw JM. Mitochondrial fusion in yeast requires the transmembrane GTPase Fzo1p. *J Cell Biol* 143: 359–373, 1998.
23. Hollenbeck PJ, Saxton WM. The axonal transport of mitochondria. *J Cell Sci* 118: 5411–5419, 2005.
24. Ichishita R, Tanaka K, Sugiura Y, Sayano T, Mihara K, Oka T. An RNAi screen for mitochondrial proteins required to maintain the morphology of the organelle in *Caenorhabditis elegans*. *J Biochem* 143: 449–454, 2008.
25. James DI, Parone PA, Mattenberger Y, Martinou JC. hFis1, a novel component of the mammalian mitochondrial fission machinery. *J Biol Chem* 278: 36373–36379, 2003.
26. Johnson D, Nehrke K. Mitochondrial fragmentation leads to intracellular acidification in *Caenorhabditis elegans* and mammalian cells. *Mol Biol Cell* 21: 2191–2201, 2010.
27. Judge AD, Sood V, Shaw JR, Fang D, McClintock K, MacLachlan I. Sequence-dependent stimulation of the mammalian innate immune response by synthetic siRNA. *Nat Biotechnol* 23: 457–462, 2005.
28. Kanazawa T, Zappaterra MD, Hasegawa A, Wright AP, Newman-Smith ED, Buttle KF, McDonald K, Mannella CA, van der Bliek AM. The *C. elegans* Opa1 homologue EAT-3 is essential for resistance to free radicals. *PLoS Genet* 4: e1000022, 2008.
29. Kumar AP, Chang MK, Fliegel L, Pervaiz S, Clement MV. Oxidative repression of NHE1 gene expression involves iron-mediated caspase activity. *Cell Death Differ* 14: 1733–1746, 2007.
30. Maleth J, Venglovecz V, Razga Z, Tiszlavicz L, Rakoncay Z Jr, Hegyi P. Non-conjugated chenodeoxycholate induces severe mitochondrial damage and inhibits bicarbonate transport in pancreatic duct cells. *Gut* 60: 136–138, 2011.
31. Marchbank NJ, Craig JE, Leek JP, Toohey M, Churchill AJ, Markham AF, Mackey DA, Toomes C, Inglehearn CF. Deletion of the OPA1 gene in a dominant optic atrophy family: evidence that haploinsufficiency is the cause of disease. *J Med Genet* 39: e47, 2002.
32. Mozdy AD, McCaffery JM, Shaw JM. Dnm1p GTPase-mediated mitochondrial fission is a multi-step process requiring the novel integral membrane component Fis1p. *J Cell Biol* 151: 367–380, 2000.
33. Nakamura U, Iwase M, Uchizono Y, Sonoki K, Sasaki N, Imoto H, Goto D, Iida M. Rapid intracellular acidification and cell death by H₂O₂ and alloxan in pancreatic beta cells. *Free Radic Biol Med* 40: 2047–2055, 2006.
34. Nehrke K. A reduction in intestinal cell pH_i due to loss of the *Caenorhabditis elegans* Na⁺/H⁺ exchanger NHX-2 increases life span. *J Biol Chem* 278: 44657–44666, 2003.
35. Nehrke K, Melvin JE. The NHX family of Na⁺-H⁺ exchangers in *Caenorhabditis elegans*. *J Biol Chem* 277: 29036–29044, 2002.
36. Nemoto S, Combs CA, French S, Ahn BH, Fergusson MM, Balaban RS, Finkel T. The mammalian longevity-associated gene product p66shc regulates mitochondrial metabolism. *J Biol Chem* 281: 10555–10560, 2006.
37. Neri D, Supuran CT. Interfering with pH regulation in tumours as a therapeutic strategy. *Nat Rev Drug Discov* 10: 767–777, 2011.
38. Orsini F, Moroni M, Contursi C, Yano M, Pelicci P, Giorgio M, Migliaccio E. Regulatory effects of the mitochondrial energetic status on mitochondrial p66Shc. *Biol Chem* 387: 1405–1410, 2006.
39. Otsuga D, Keegan BR, Brisch E, Thatcher JW, Hermann GJ, Bleazard W, Shaw JM. The dynamin-related GTPase, Dnm1p, controls mitochondrial morphology in yeast. *J Cell Biol* 143: 333–349, 1998.
40. Park S, Ahn JY, Lim MJ, Kim MH, Yun YS, Jeong G, Song JY. Sustained expression of NADPH oxidase 4 by p38 MAPK-Akt signaling potentiates radiation-induced differentiation of lung fibroblasts. *J Mol Med* 88: 807–816.
41. Pedrosa R, Villar VA, Pascua AM, Simao S, Hopfer U, Jose PA, Soares-da-Silva P. H₂O₂ stimulation of the Cl⁻/HCO₃⁻ exchanger by angiotensin II and angiotensin II type 1 receptor distribution in membrane microdomains. *Hypertension* 51: 1332–1338, 2008.
42. Pfeiffer J, Johnson D, Nehrke K. Oscillatory transepithelial H⁺ flux regulates a rhythmic behavior in *C. elegans*. *Curr Biol* 18: 297–302, 2008.
43. Pouyssegur J, Sardet C, Franchi A, L'Allemain G, Paris S. A specific mutation abolishing Na⁺/H⁺ antiport activity in hamster fibroblasts precludes growth at neutral and acidic pH. *Proc Natl Acad Sci USA* 81: 4833–4837, 1984.
44. Santel A, Fuller MT. Control of mitochondrial morphology by a human mitofusin. *J Cell Sci* 114: 867–874, 2001.
45. Shepard KA, Yaffe MP. The yeast dynamin-like protein, Mgm1p, functions on the mitochondrial outer membrane to mediate mitochondrial inheritance. *J Cell Biol* 144: 711–720, 1999.
46. Simao S, Fraga S, Jose PA, Soares-da-Silva P. Oxidative stress and alpha1-adrenoceptor-mediated stimulation of the Cl⁻/HCO₃⁻ exchanger in immortalized SHR proximal tubular epithelial cells. *Br J Pharmacol* 153: 1445–1455, 2008.
47. Sipos H, Torocsik B, Tretter L, Adam-Vizi V. Impaired regulation of pH homeostasis by oxidative stress in rat brain capillary endothelial cells. *Cell Mol Neurobiol* 25: 141–151, 2005.
48. Sledzinski Z, Wozniak M, Antosiewicz J, Lezoch E, Familiari M, Bertoli E, Greci L, Brunelli A, Mazera N, Wajda Z. Protective effect of 4-hydroxy-TEMPO, a low molecular weight superoxide dismutase mimic, on free radical toxicity in experimental pancreatitis. *Int J Pancreatol* 18: 153–160, 1995.
49. Smirnova E, Shurland DL, Ryazantsev SN, van der Bliek AM. A human dynamin-related protein controls the distribution of mitochondria. *J Cell Biol* 143: 351–358, 1998.
50. Soenen SJ, Brisson AR, De Cuyper M. Addressing the problem of cationic lipid-mediated toxicity: the magnetoliposome model. *Biomaterials* 30: 3691–3701, 2009.
51. Strayer A, Wu Z, Christen Y, Link CD, Luo Y. Expression of the small heat-shock protein Hsp16–2 in *Caenorhabditis elegans* is suppressed by Ginkgo biloba extract EGB 761. *FASEB J* 17: 2305–2307, 2003.
52. Thomas JA, Buchsbaum RN, Zimniak A, Racker E. Intracellular pH measurements in Ehrlich ascites tumor cells utilizing spectroscopic probes generated in situ. *Biochemistry* 18: 2210–2218, 1979.
53. Trnka J, Blaikie FH, Smith RA, Murphy MP. A mitochondria-targeted nitroxide is reduced to its hydroxylamine by ubiquinol in mitochondria. *Free Radic Biol Med* 44: 1406–1419, 2008.
54. Twig G, Elorza A, Molina AJ, Mohamed H, Wikstrom JD, Walzer G, Stiles L, Haigh SE, Katz S, Las G, Alroy J, Wu M, Py BF, Yuan J, Deeney JT, Corkey BE, Shirihai OS. Fission and selective fusion govern mitochondrial segregation and elimination by autophagy. *EMBO J* 27: 433–446, 2008.
55. Wang W, Fang H, Groom L, Cheng A, Zhang W, Liu J, Wang X, Li K, Han P, Zheng M, Yin J, Wang W, Mattson MP, Kao JP, Lakatta EG, Sheu SS, Ouyang K, Chen J, Dirksen RT, Cheng H. Superoxide flashes in single mitochondria. *Cell* 134: 279–290, 2008.
56. Wu RF, Ma Z, Liu Z, Terada LS. Nox4-derived H₂O₂ mediates endoplasmic reticulum signaling through local Ras activation. *Mol Cell Biol* 30: 3553–3568.
57. Yoon Y, Krueger EW, Oswald BJ, McNiven MA. The mitochondrial protein hFis1 regulates mitochondrial fission in mammalian cells through an interaction with the dynamin-like protein DLP1. *Mol Cell Biol* 23: 5409–5420, 2003.
58. Zuchner S, Mersyanova IV, Muglia M, Bissar-Tadmouri N, Rochelle J, Dadali EL, Zappia M, Nelis E, Patitucci A, Senderek J, Parman Y, Evgrafov O, Jonghe PD, Takahashi Y, Tsuji S, Pericak-Vance MA, Quattrone A, Battaloglu E, Polyakov AV, Timmerman V, Schroder JM, Vance JM. Mutations in the mitochondrial GTPase mitofusin 2 cause Charcot-Marie-Tooth neuropathy type 2A. *Nat Genet* 36: 449–451, 2004.